RECENT RESULTS OF FUSION INDUCED BY NEUTRON-RICH RADIOACTIVE BEAMS STUDIED AT HRIBF*

J.F. Liang

Joint Institute for Heavy Ion Research, Oak Ridge National Laboratory
Oak Ridge, Tennessee 37831, USA

(Received November 19, 2012)

The reaccelerated fission-fragment beams at HRIBF provide a unique opportunity for studying the mechanisms of fusion involving nuclei with large neutron excess. The fusion excitation functions for neutron-rich radioactive ^{132}Sn incident on ^{40}Ca and ^{58}Ni targets have been measured to explore the role of transfer couplings in sub-barrier fusion enhancement. Evaporation residue cross sections for ^{124,126,127,128}Sn+^{64}Ni were measured to study the dependence of fusion probability on neutron excess.

DOI:10.5506/APhysPolB.44.427
PACS numbers: 25.60.–t, 25.60.Pj, 25.70.–z, 25.70.Gh

1. Introduction

Fusion induced by radioactive beams has been an active area of research in recent years [1, 2]. The fusion rate is expected to increase at energies near and below the Coulomb barrier due to the larger r.m.s. radius of the unstable nuclei, the excitations of collective modes, and nucleon transfer. It has been shown that large sub-barrier fusion enhancement correlates with the presence of positive Q-value transfer channels [3, 4]. The effects of coupling to nucleon transfer is expected to be significant for reactions involving radioactive nuclei because, for some projectile and target combinations, there are a large number of nucleon transfer channels with positive Q-values. The couplings to these transfer reactions could result in substantially enhanced fusion cross sections at sub-barrier energies.

Neutron-rich radioactive beams may be used for synthesizing isotopes of heavy elements. These beams may help reach the predicted $N = 184$ neutron shell closure [5]. Moreover, the fusion of neutron-rich radioactive

* Presented at the Zakopane Conference on Nuclear Physics "Extremes of the Nuclear Landscape", Zakopane, Poland, August 27–September 2, 2012.

nuclei in the crust of neutron stars may play an important role in the energy generation and distribution in neutron stars [6]. Therefore, it is important to understand the reaction mechanisms of fusion induced by neutron-rich nuclei.

2. Fusion of ^{124,132}Sn+^{40,48}Ca

The sub-barrier fusion cross sections for ^{40}Ca+^{96}Zr were much enhanced compared to ^{40}Ca+^{90}Zr [3]. Coupled-channels calculations considering the excitation of the projectile and target were able to reproduce the fusion excitation function for ^{40}Ca+^{90}Zr but underpredict that for ^{40}Ca+^{96}Zr. The sub-barrier fusion enhancement for ^{40}Ca+^{96}Zr was attributed to the couplings to neutron transfer because the Q-values for up to 9 neutrons transferring from ^{96}Zr to ^{40}Ca are positive. In contrast, the Q-values for neutron transfer are negative for ^{40}Ca+^{90}Zr. A subsequent measurement of the fusion of ^{40}Ca+^{94}Zr supported the conclusion [7]. The fusion excitation functions for ^{40}Ca+^{94,96}Zr were measured to high precision which allowed deducing the barrier distributions. A tail of the low energy barrier extends to energies well below the uncoupled barrier for ^{40}Ca+^{94,96}Zr but is absent in ^{40}Ca+^{90}Zr. This tail is considered the fingerprint for coupling to positive Q-value channels.

The fusion of ^{40}Ca+^{124}Sn was measured by Scarlassara *et al.* [4] at Legnaro and large sub-barrier fusion enhancement was observed. Because the Q-values for transferring 2 to 11 neutrons from ^{124}Sn to ^{40}Ca are positive, the large sub-barrier fusion enhancement was attributed to the coupling to transfer, similar to the fusion of ^{40}Ca+^{96}Zr. Doubly magic ^{132}Sn has eight extra neutrons compared to ^{124}Sn. The number of open channels for neutron transfer is larger in ^{40}Ca+^{132}Sn than in ^{40}Ca+^{124}Sn. The Q-values for neutron transfer in ^{40}Ca+^{132}Sn are larger, too. The sub-barrier fusion of ^{40}Ca+^{132}Sn is expected to be enhanced due to the coupling to transfer.

The fusion of ^{124,132}Sn+^{40,48}Ca were measured in inverse kinematics at the Holifield Radioactive Ion Beam Facility (HRIBF) using the apparatus described in Ref. [8]. The fusion excitation function for ^{124}Sn+^{40}Ca is in good agreement with Scarlassara *et al.*'s measurement. The fusion cross sections as a function of the reaction energy for the four reactions are shown in Fig. 1. The excitation functions are compared in reduced scale where the differences in nuclear size ($R_\circ^2$) and barrier height ($B_\circ$) are factored out for the cross section and center-of-mass energy, respectively. A simple scaling method was used here with $R_\circ = A_{\rm P}^{1/3} + A_{\rm T}^{1/3}$ and $B_\circ = Z_{\rm P}Z_{\rm T}/R_\circ$, where $A_{\rm P}$ ($A_{\rm T}$) and $Z_{\rm P}$ ($Z_{\rm T}$) are the mass and atomic number of the projectile (target), respectively. The dotted curve is the result of a one-dimensional barrier penetration model prediction. All four reactions exhibit fusion enhancement at energies below the barrier. The sub-barrier enhancement is larger for reactions involving ^{40}Ca. For reactions with the same Ca isotope, the sub-barrier fusion rate is higher for the ^{124}Sn induced reaction than the ^{132}Sn induced reaction. This trend coincides with the fact that ^{132}Sn is doubly magic and less collective than ^{124}Sn. Therefore, the influence of coupling to the inelastic excitation of Sn on sub-barrier fusion enhancement is larger for ^{124}Sn+Ca than for ^{132}Sn+Ca.

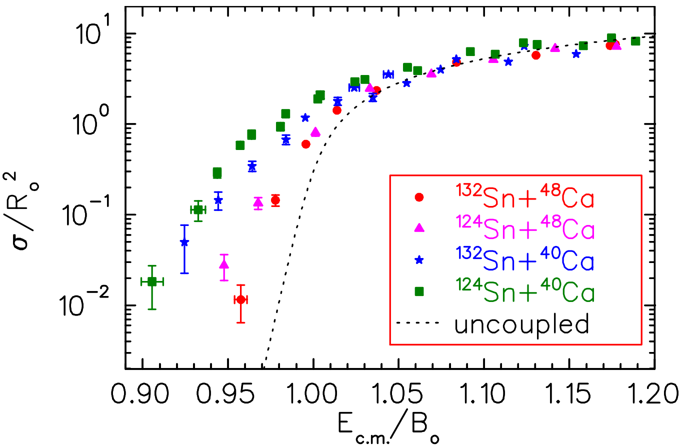

Fig. 1. Reduced fusion cross sections for ^{124,132}Sn+^{40,48}Ca are displayed as a function of reduced energy in the center-of-mass. The nuclear size and the barrier height are factored out for the cross section and the energy, respectively. The dotted curve is the result of a one-dimensional barrier penetration calculation. The circles are for ^{132}Sn+^{48}Ca, the triangles are for ^{124}Sn+^{48}Ca, the stars are for ^{132}Sn+^{40}Ca, and the squares are for ^{124}Sn+^{40}Ca.

Coupled-channels calculations considering the excitations of the projectile and target are able to reproduce the fusion excitation function for ^{124}Sn+^{48}Ca but underpredict the sub-barrier cross sections for ^{124,132}Sn+^{40}Ca [9]. The Q-values for neutron transfer in the reactions with ^{48}Ca are negative whereas there are positive Q-value transfer channels in the reactions with ^{40}Ca. The large sub-barrier fusion enhancement in ^{132}Sn+^{40}Ca can be attributed to the couplings to neutron transfer just like ^{40}Ca+^{124}Sn and ^{40}Ca+^{96}Zr [9].

3. Fusion of ^{132}Sn+^{58}Ni

To further explore the effects of transfer couplings, measurements of the fusion excitation function for ^{132}Sn+^{58}Ni were performed at HRIBF with ^{132}Sn beams [10]. The Q-values for neutron transfer is larger than those in

^{132}Sn+^{40}Ca. The reduced fusion excitation functions for ^{124,132}Sn+^{58,64}Ni are compared in Fig. 2. The fusion cross sections for ^{124}Sn+^{58,64}Ni are obtained from Ref. [11]. Because the compound nucleus is heavier and the reaction is more mass-symmetric, fusion hindrance due to quasifission reduces the fusion cross sections at high energies for the neutron deficient ^{124}Sn+^{58}Ni reaction. The four reduced excitation functions, ^{124,132}Sn+^{58,64}Ni, overlap in the sub-barrier region even though the Q-values for neutron transfer differ significantly among these reactions. This behavior is dramatically different from the comparison among the ^{124,132}Sn+^{40,48}Ca reactions. Furthermore, the Sn+Ni excitation functions overlap with the reference reaction, ^{132}Sn+^{48}Ca, which has no positive Q-values for transfer, as shown in Fig. 2. The sub-barrier fusion enhancement for ^{132}Sn+^{40}Ca is much larger than that for Sn+Ni.

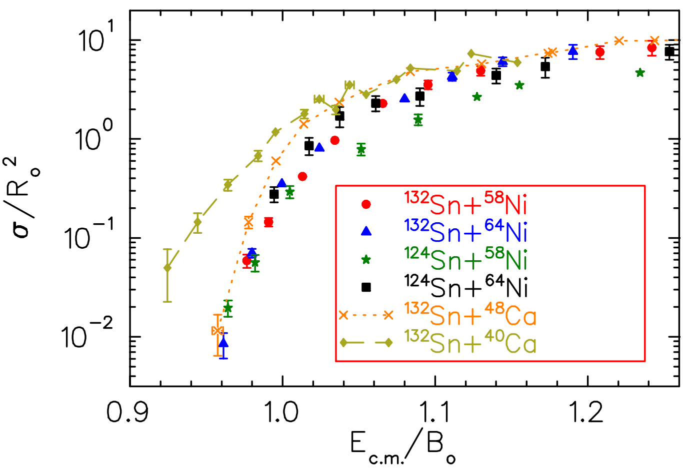

Fig. 2. Reduced fusion cross sections for ^{124,132}Sn+^{58,64}Ni are displayed as a function of reduced energy in the center-of-mass. The nuclear size and the barrier height are factored out for the cross section and the energy, respectively. The circles are for ^{132}Sn+^{58}Ni, the triangles are for ^{132}Sn+^{64}Ni, the stars are for ^{124}Sn+^{58}Ni, and the squares are for ^{124}Sn+^{64}Ni. The excitation functions for ^{132}Sn+^{40,48}Ca are shown by the diamonds and crosses for comparisons.

4. Fusion of ^{48}Ti+^{124}Sn

It is puzzling that the sub-barrier fusion enhancement due to the coupling to neutron transfer is very pronounced in ^{132}Sn+^{40}Ca but absent in ^{132}Sn+^{58}Ni. The Q-values for ground state to ground state multineutron transfer are similar between the two reactions, as shown in Fig. 3.

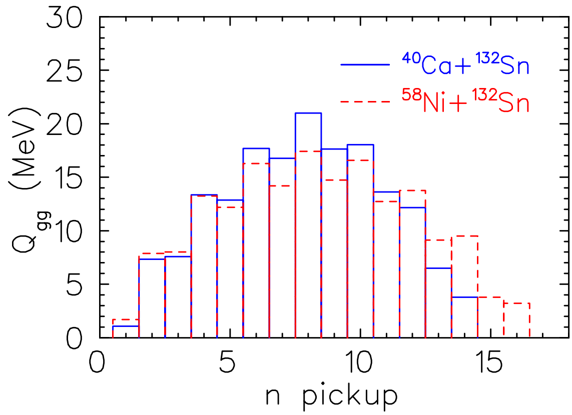

Fig. 3. Q-values for ground state to ground state neutron transfer for ^{132}Sn+^{58}Ni (dashed lines) and ^{132}Sn+^{40}Ca (solid lines).

Some of the differences for the two reaction systems, ^{124,132}Sn+^{40}Ca and ^{124,132}Sn+^{58}Ni, that may contribute to the observed differences in sub-barrier fusion enhancement are discussed below.

- The product of the atomic number for the projectile and target, $Z_{\mathrm{P}}Z_{\mathrm{T}}$ is 1000 for Sn+Ca and 1400 for Sn+Ni. The rate of deep inelastic collisions becomes higher for Sn+Ni because of the larger $Z_{\mathrm{P}}Z_{\mathrm{T}}$. This may influence the fusion yield at energies below the barrier [12].

- The open orbitals for neutrons transferred from ^{132}Sn to ^{40}Ca are $f_{7/2}$ and above whereas the open orbitals for neutrons transferred to ^{58}Ni are $p_{3/2}$ and above. The transfer form factor is a function of the angular momentum of the initial and final states. As a result, the strength for the transfer couplings would be different for the two reactions.

- The ^{40}Ca nucleus has a very collective octupole state, $E^* = 3.74$ MeV. The coupling to the excitation to this state can renormalize the potential and may result in a lowered barrier [13].

To investigate the differences in sub-barrier fusion enhancement in Sn+^{40}Ca and Sn+^{58}Ni and the couplings to transfer, the fusion excitation functions for ^{124}Sn+^{46,50}Ti have been measured at HRIBF. The ^{124}Sn+^{46}Ti reaction bares some similarities to ^{124}Sn+^{40}Ca. The $Z_{\mathrm{P}}Z_{\mathrm{T}}$ is 1100 and the neutrons transferred from ^{124}Sn to ^{46}Ti can populate the $f_{7/2}$ orbital and above. However, the octupole state of ^{46}Ti is much less collective than ^{40}Ca but similar to ^{58}Ni.

Figure 4 presents the reduced fusion excitation function for ^{124}Sn+^{46}Ti and the comparison with that for ^{124}Sn+^{40}Ca. The excitation functions for ^{124}Sn+^{48}Ca and ^{124}Sn+^{50}Ti are shown for comparison as well. The latter two reactions do not have positive Q-values for neutron transfer. The sub-barrier fusion enhancement is comparable for these two reactions and is smaller than ^{124}Sn+^{46}Ti and ^{124}Sn+^{40}Ca. For ^{124}Sn+^{46}Ti, the sub-barrier fusion enhancement is smaller than ^{124}Sn+^{40}Ca even though the Q-values for ground state to ground state neutron transfer are similar. The slope of the cross section falls off at a slower rate for ^{124}Sn+^{46}Ti than ^{124}Sn+^{40}Ca at sub-barrier energies. This suggests that the effect of coupling to positive Q-value channels is larger in ^{124}Sn+^{46}Ti.

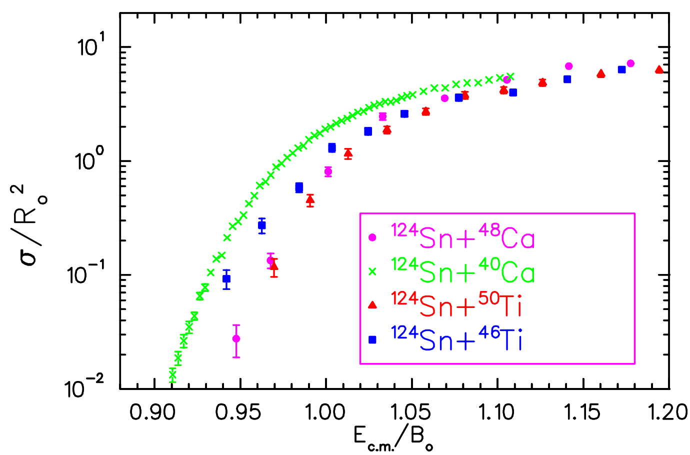

Fig. 4. Fusion excitation functions for ^{124}Sn+^{46,50}Ti and ^{124}Sn+^{40,48}Ca are compared in reduced scales where the nuclear size and the barrier height are factored out. The circles are for ^{124}Sn+^{48}Ca [9], the crosses are for ^{124}Sn+^{40}Ca [4], the triangles are for ^{124}Sn+^{50}Ti, and the squares are for ^{124}Sn+^{46}Ti.

It is necessary to inspect the details of the reaction mechanisms in order to gain insight into the differences observed among these reactions. A high precision measurement of the fusion excitation function for ^{124}Sn+^{46}Ti was carried out at the Australian National University (ANU). The ^{46}Ti beams were accelerated by the 14UD tandem accelerator and incident on a ^{124}Sn target. The evaporation resides were transported by the gas-filled superconducting solenoid (SOLITAIRE) and detected by two multiwire proportional counters at and behind the focal plane [14]. The fusion excitation function was measured at an energy step of 1 MeV in the center-of-mass frame. A preliminary analysis shows that the barrier distribution deduced for ^{46}Ti+^{124}Sn has a low energy barrier about 3% below the uncoupled barrier which is obtained from the Broglia–Winther systematics [15]. In contrast, the barrier distribution for ^{40}Ca+^{124}Sn has a low energy barrier at 5% below the uncoupled barrier and the tail falls off more steeply than that for ^{46}Ti+^{124}Sn. This is a hint that the coupling to transfer may be more important in ^{46}Ti+^{124}Sn. The large sub-barrier fusion enhancement in ^{40}Ca+^{124}Sn may be explained by potential renormalization.

Qualitative comparisons of the barrier distributions predicted by the coupled-channels code CCFULL [16] are made for the three reactions ^{40}Ca+^{124}Sn, ^{48}Ti+^{124}Sn, and ^{58}Ni+^{124}Sn. Because all three reactions share a common nucleus ^{124}Sn, the coupling to the inelastic excitations to the first 2^+ and 3^- states of the other reaction partners is compared in Fig. 5. The nuclear structure properties of the excited 2^+ and 3^- states were obtained from Raman [17] and Spears [18], respectively. As can be seen, the coupling to the excitation of the octupole state in ^{40}Ca produces a low energy barrier 4% below the uncoupled barrier and the barrier distribution is dominated by the coupling to the 3^- state. For the other two reactions, the low energy barrier is only 2% below the uncoupled barrier. Therefore, the coupling to the inelastic excitation of the octupole state in ^{40}Ca plays a major role in enhancing the fusion of ^{40}Ca+^{124}Sn at sub-barrier energies. It is conceivable that the couplings to inelastic excitations and neutron transfer result in the large sub-barrier fusion enhancement observed in ^{40}Ca+^{124}Sn with coupling to the 3^- state in ^{40}Ca playing a major role.

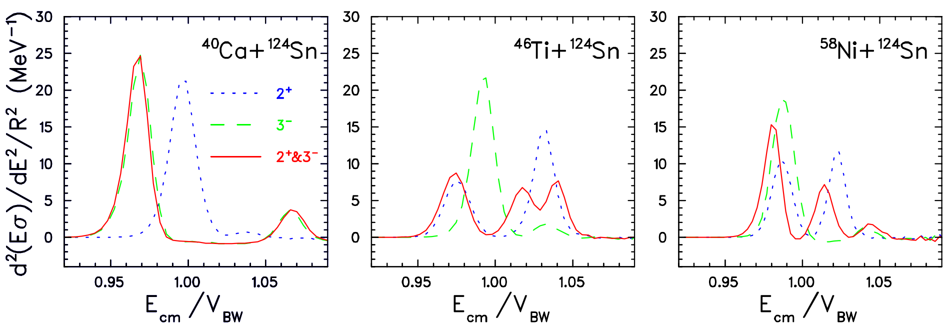

Fig. 5. Barrier distributions deduced from coupled-channels calculations for ^{124}Sn+^{40}Ca, ^{124}Sn+^{58}Ni, and ^{124}Sn+^{46}Ti.

5. Fusion probability

Fusion hindrance in heavy systems is attributed to quasifission where the reacting nuclei overcome the Coulomb barrier but fail to pass inside the saddle point, and reseparate into large mass fragments. It is important to get a better understanding of this process in order to reliably predict the production cross section for superheavy elements. In particular, the role played by neutron excess in affecting fusion hindrance is not well understood.

Sahm *et al.* [19] have defined the angular momentum averaged fusion probability as

$$\langle P_{\rm CN}\rangle = \frac{\sigma_{\rm ER}}{\sigma_{\rm ER}^{(\circ)}}\,,$$

where $\sigma_{\rm ER}^{(\circ)}$ is the maximum evaporation residue cross section for a given excitation energy. This corresponds to the evaporation residue cross section for $P_{\rm CN} = 1$. Therefore, it can be calculated by a statistical model without considering fusion hindrance, such as PACE2 [20]. Figure 6 shows the ratio of the measured $\sigma_{\rm ER}$ to the calculated $\sigma_{\rm ER}^{(\circ)}$ as a function of the effective fissility parameter. The fusion probability is comparable among all the reactions. There may be a hint of increasing fusion probability with increasing neutron excess in Sn [21]. Further measurements using more neutron-rich Sn isotopes would be useful for determining the dependence of fusion probability on neutron excess.

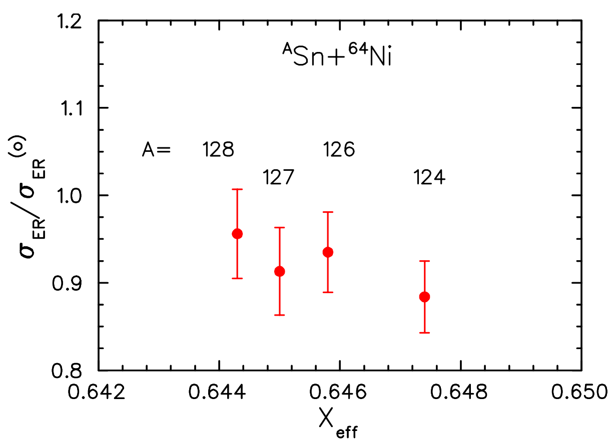

Fig. 6. The fusion probability for ^{124,126,127,128}Sn+^{64}Ni obtained by taking the ratio of the measured evaporation residue cross section to that calculated by PACE2 is plotted as a function of the effective fissility parameter.

6. Summary and conclusions

Fusion excitation functions have been measured using neutron-rich radioactive ^{132}Sn beams incident on ^{40}Ca and ^{58}Ni targets. The sub-barrier fusion enhancement for ^{132}Sn+^{40}Ca is larger than that for ^{132}Sn+^{58}Ni although the neutron transfer Q-values are similar for the two reactions. To further explore the coupling to neutron transfer, the fusion excitation function for ^{46}Ti+^{124}Sn has been measured to high precision. The barrier distributions deduced from the excitation functions suggest that the large sub-barrier fusion enhancement in ^{132}Sn+^{40}Ca may be the result of coupling to neutron transfer and inelastic excitations of the projectile and target with the coupling to the octupole state in ^{40}Ca playing a major role.

The fusion probability for ^{124,126,127,128}Sn+^{64}Ni seems to increase with increasing neutron excess in Sn. The present results suggest that fusion hindrance would not increase in superheavy element synthesis using reactions induced by neutron-rich radioactive beams, leading to a hope that neutron-rich radioactive beams may one day be useful in the production of isotopes of superheavy elements.

The author wishes to thank J.M. Allmond, C.J. Gross, Z. Kohley, K. Lagergren, P.E. Mueller, D. Shapira, R.L. Varner (ORNL), A.L. Caraley (SUNY at Oswego), J.J. Kolata, A. Roberts, A. Howard (Notre Dame), W. Loveland (Oregon State) for collaborating on measurements at HRIBF, and M. Dasgupta, D.J. Hinde, E. Williams, M.L. Brown, I.P. Carter, M. Evers, D.H. Luong, A. Wakhle (ANU) for collaborating on measurements at ANU. Research at HRIBF was supported by the Office of Nuclear Physics, U.S. Department of Energy.

REFERENCES

[1] J.F. Liang, C. Signorini, *Int. J. Mod. Phys.* **E14**, 1121 (2005).

[2] N. Keeley, R. Raabe, N. Alamanos, J.L. Sida, *Prog. Part. Nucl. Phys.* **59**, 579 (2007).

[3] H. Timmers *et al.*, *Nucl. Phys.* **A633**, 421 (1998).

[4] F. Scarlassara *et al.*, *Nucl. Phys.* **A672**, 99 (2000).

[5] W. Loveland, *Phys. Rev.* **C76**, 069801 (2007).

[6] C.J. Horowitz, H. Dussan, D.K. Berry, *Phys. Rev.* **C77**, 045807 (2008).

[7] A.M. Stefanini *et al.*, *Phys. Rev.* **C76**, 014610 (2007).

[8] D. Shapira *et al.*, *Nucl. Instrum. Methods Phys. Res.* **A551**, 330 (2005).

[9] J.J. Kolata *et al.*, *Phys. Rev.* **C85**, 054603 (2012).

[10] Z. Kohley *et al.*, *Phys. Rev. Lett.* **107**, 202701 (2011).

[11] K.T. Lesko *et al.*, *Phys. Rev.* **C34**, 2155 (1986).

[12] F.L.H. Wolfs, *Phys. Rev.* **C36**, 1379 (1987).

[13] M. Trotta *et al.*, *Phys. Rev.* **C65**, 011601(R) (2001).

[14] M.D. Rodrígues *et al.*, *Nucl. Instrum. Methods Phys. Res.* **A614**, 119 (2010).

[15] R.A. Broglia, A. Winther, *Heavy Ion Reactions*, Frontiers in Physics Lecture Series, Vol. 84, Addison-Wesley, Redwood, CA, 1991.

[16] K. Hagino, N. Rowley, A.T. Kruppa, *Comput. Phys. Commun.* **123**, 143 (1999).

[17] S. Raman *et al.*, *At. Data Nucl. Data Tables* **36**, 1 (1978).
[18] R.H. Spear, *At. Data Nucl. Data Tables* **42**, 55 (1989).
[19] C.-C. Sahm *et al.*, *Nucl. Phys.* **A441**, 316 (1985).
[20] A. Gavron, *Phys. Rev.* **C21**, 230 (1980).
[21] J.F. Liang *et al.*, *Phys. Rev.* **C85**, 031601(R) (2012).